NAM-UK, Manchester 27-30 March 2012

Line-of-sight geometrical effects on intensity perturbations by sausage modes

Patrick Antolin, Tom Van Doorsselaere

Centre for Plasma Astrophysics, KU Leuven, Belgium

Outline

- Introduction - a heated debate in the solar community
- Model
  - MHD sausage mode in ideal cylindrical tube
- Results (aiming Imaging and Spectroscopic instruments)
  - Effect of l.o.s. angle
  - Effect of spatial resolution
- Conclusions

Introduction

- Waves are ubiquitous in the solar atmosphere (Tomczyk et al. 2007, Okamoto et al. 2007, De Moortel et al. 2000, McIntosh et al. 2011, ...)

- Measuring their properties with imaging and spectroscopic instruments allows the determination of the in-situ plasma conditions: coronal seismology (Nakariakov & Verwichte 2005, De Moortel & Nakariakov 2012).

- For this purpose their correct interpretation is essential (De Pontieu et al 2007, Erdelyi & Fedun 2007, Van Doorsselaere et al 2008,...).

➡Necessity for determining the observational signatures of MHD modes: forward modeling (Cooper et al 2003, Williams 2004, Antolin et al. 2008, Taroyan & Erdelyi 2009, De Moortel & Pascoe 2012, Gruszecki et al. 2012).

OBJECTIVE: Determine the line-of-sight geometrical effects on wave observations concentrating first on the sausage mode.

Model

- Ideal axisymmetric plasma cylinder with sausage mode, described by (Edwin & Roberts 1983):

$$\frac{d^2P'}{dr^2} + \frac{1}{r}\frac{dP'}{dr} - \kappa^2 P' = 0,$$

$$\rho(\omega^2 - k^2 C_A^2)V_r = -i\omega\frac{dP'}{dr},$$

$$\rho(\omega^2 - k^2 C_A^2)V_\phi = 0,$$

$$\rho(\omega^2 - k^2 C_T^2)V_z = \omega k \frac{C_s^2}{C_s^2 + C_A^2} P'$$

P': total pressure perturbation

$$\kappa^2 = \frac{(k^2 C_s^2 - w^2)(k^2 C_A^2 - w^2)}{(C_s^2 + C_A^2)(k^2 C_T^2 - w^2)}, C_T^2 = \frac{C_s^2 C_A^2}{C_s^2 + C_A^2}$$

ω solution of the dispersion relation:

$$\frac{\kappa_e}{\varrho_e(k^2 C_{Ae}^2 - \omega^2)}\frac{K_0'(\kappa_e w)}{K_0(\kappa_e w)} = \frac{\sqrt{-\kappa_i^2}}{\varrho_i(k^2 C_{Ai}^2 - \omega^2)}\frac{J_0'(\sqrt{-\kappa_i^2}w)}{J_0(\sqrt{-\kappa_i^2}w)}$$

- Low β-plasma. Density contrast ρ_e/ρ_i = 0.6, Magnetic field variation B_e/B_i = 1.7, wavenumber = 3.6/R
- Sausage mode: essentially compressible and transverse. Emission in Fe IX coronal line (171.07 Å) (CHIANTI, Dere et al. 2009)

Model

A slice along the axis of the tube

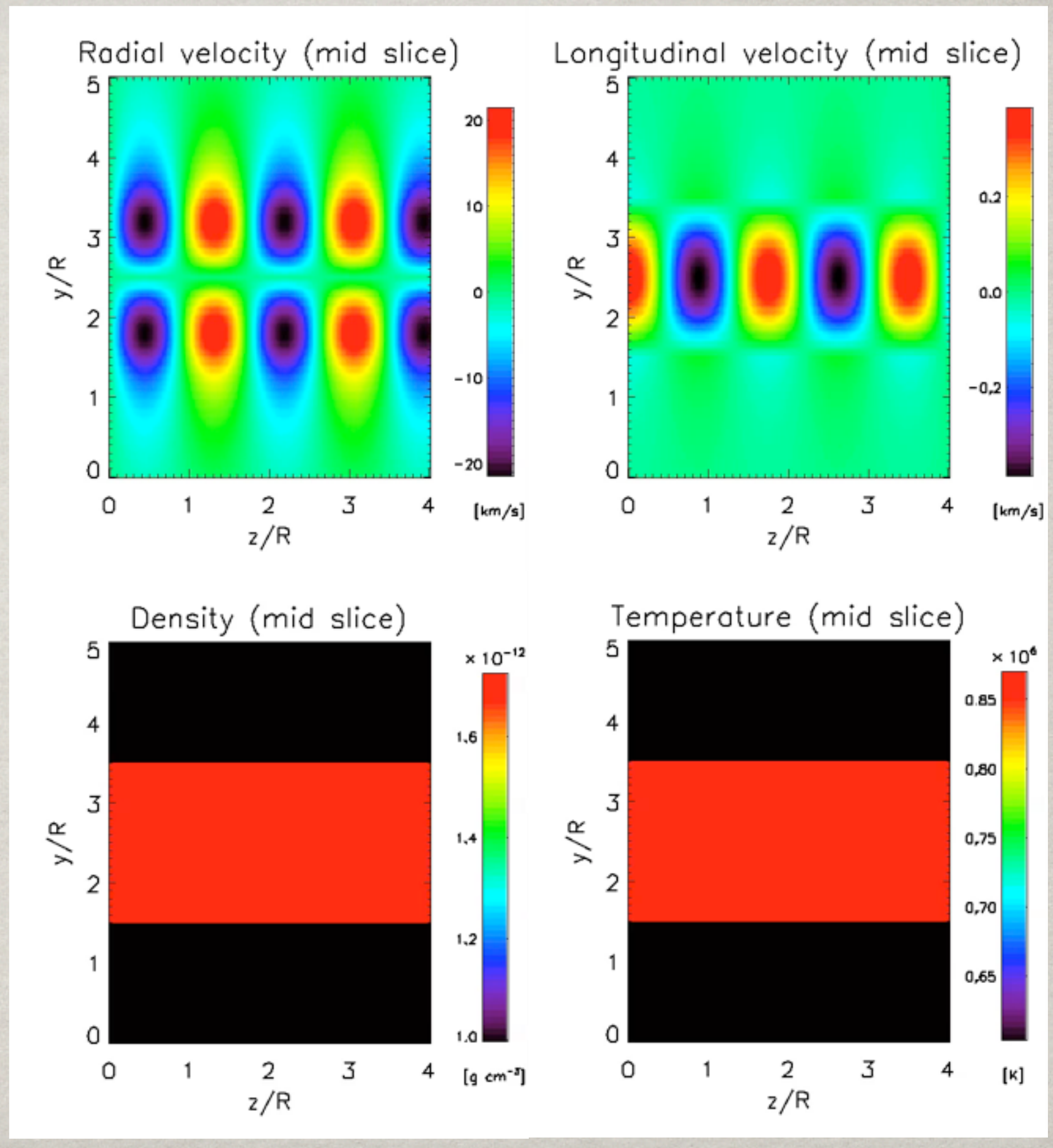

Model

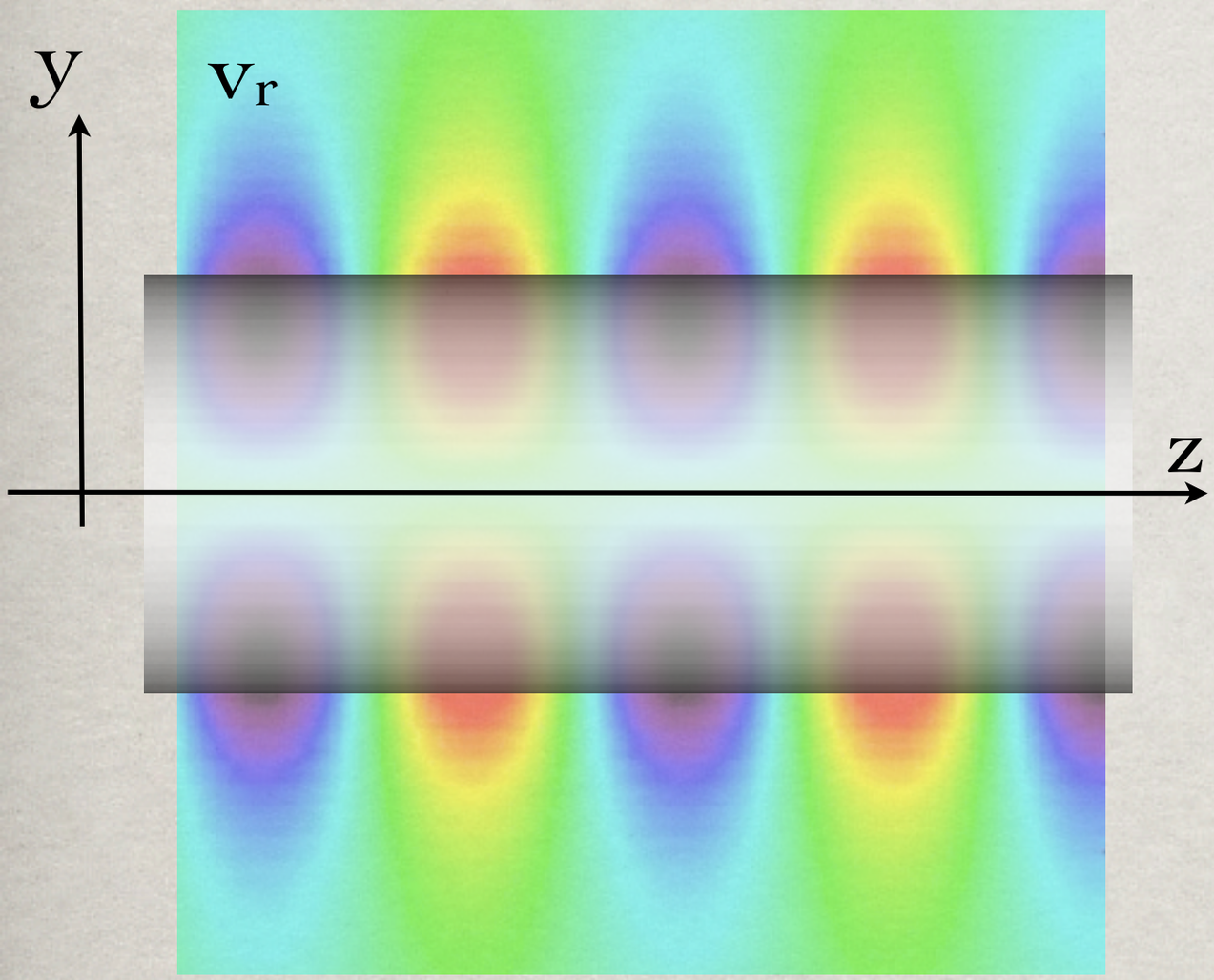

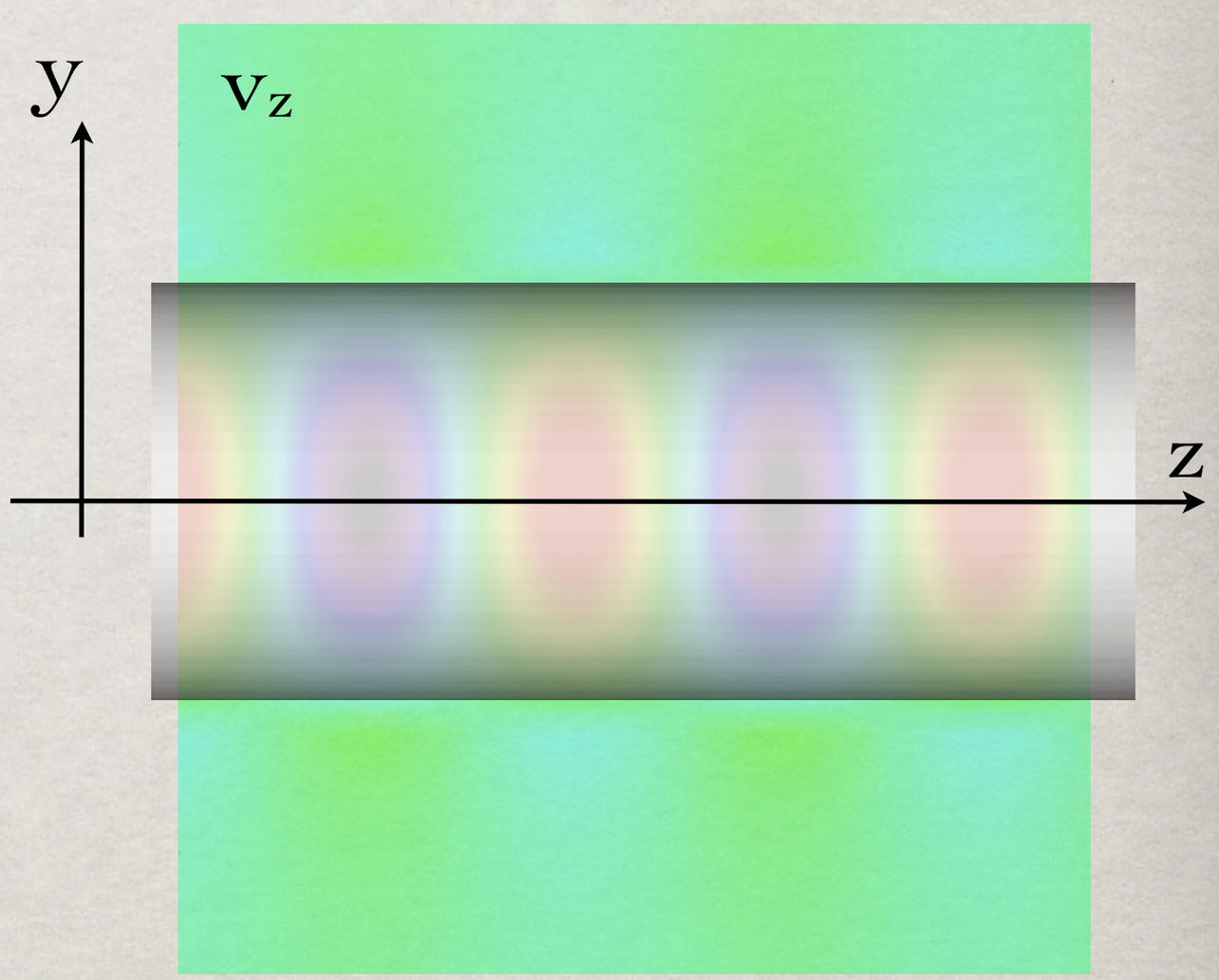

- Different viewing angles (rays): 0°, 30°, 45°, 60°
- For each ray we consider different spatial resolution: 1 pixel (0R), 1 radius (1R), 3 radiuses (3R)

Model

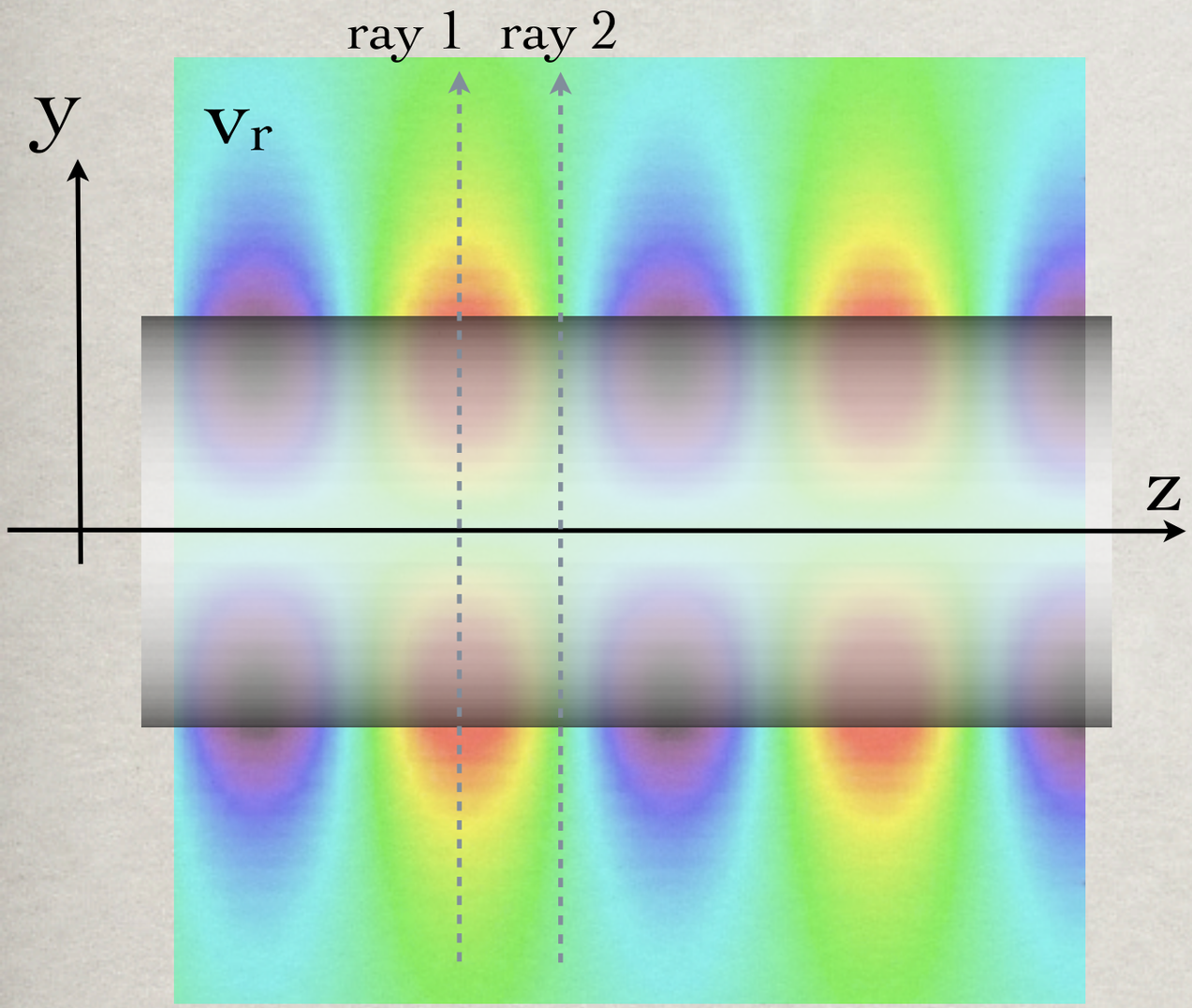

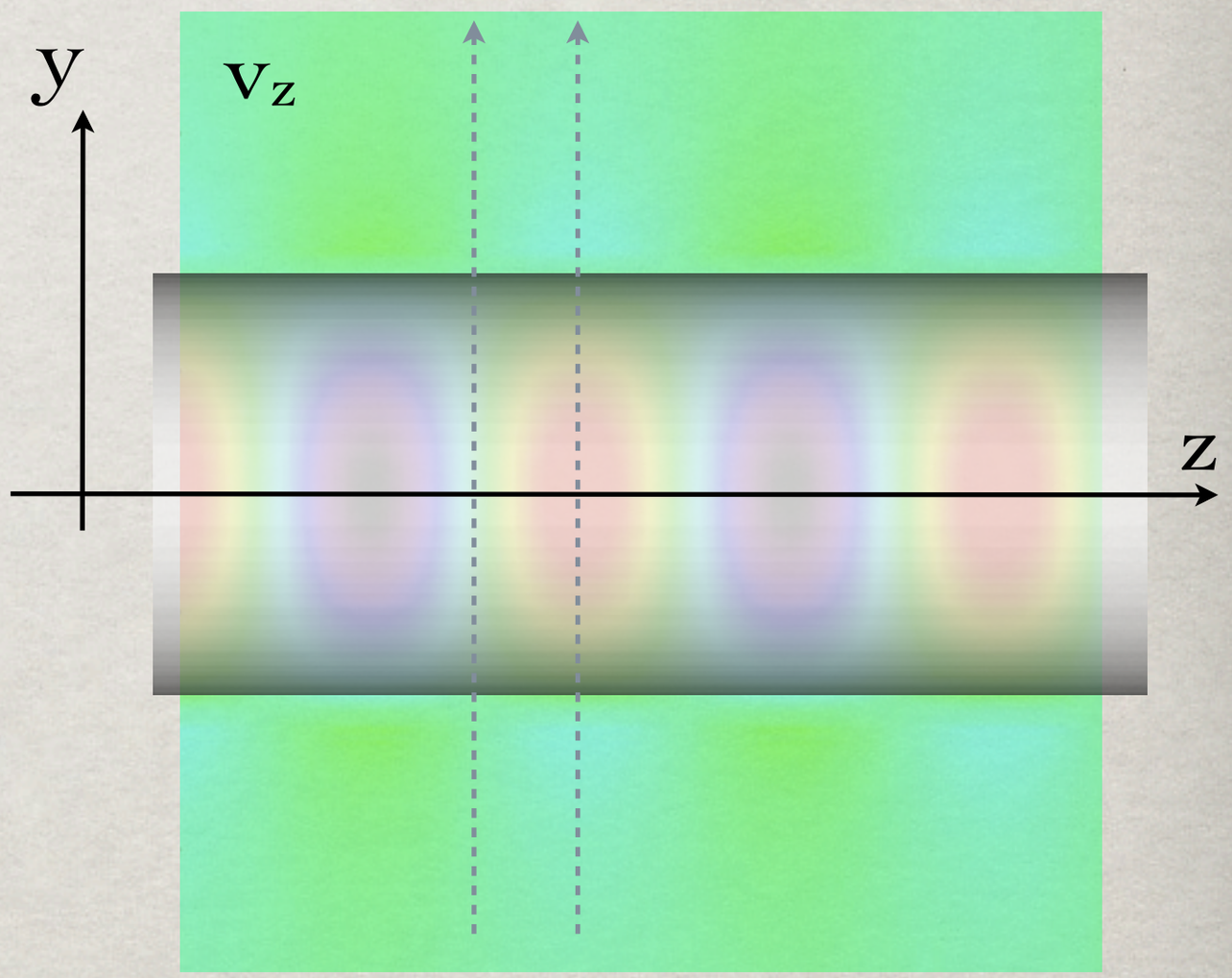

0° angle

- Different viewing angles (rays): 0°, 30°, 45°, 60°
- For each ray we consider different spatial resolution: 1 pixel (0R), 1 radius (1R), 3 radiuses (3R)

Model

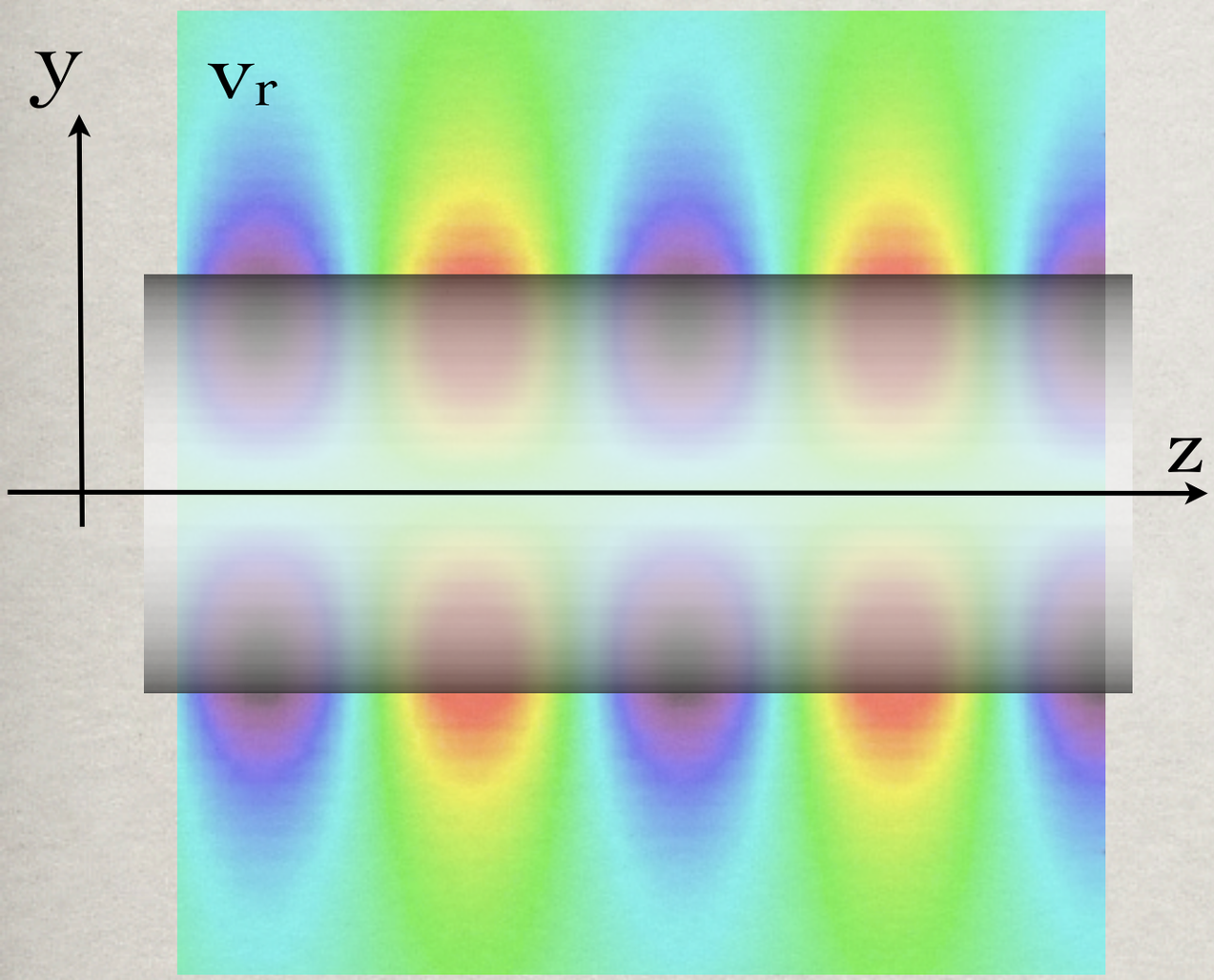

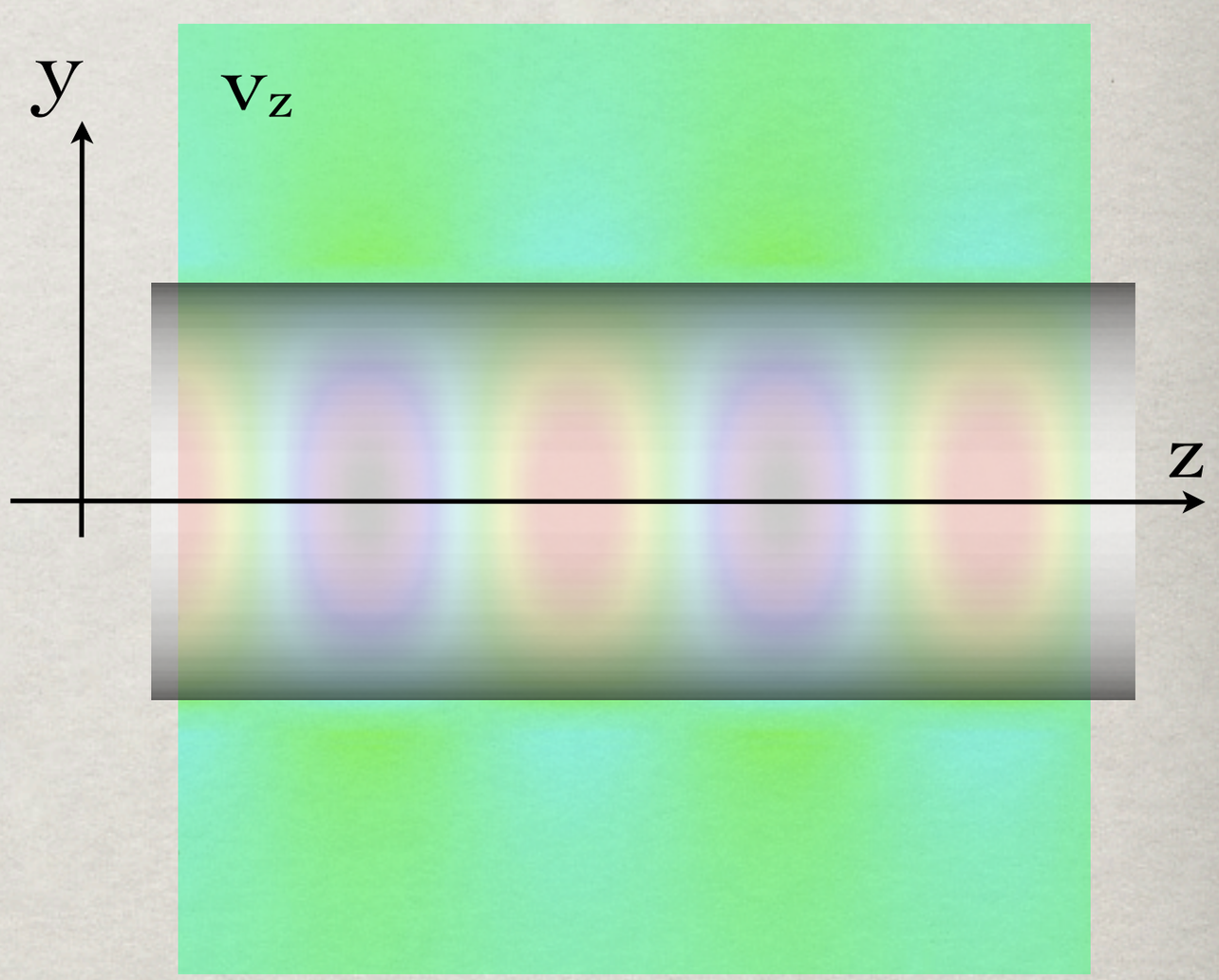

- Different viewing angles (rays): 0°, 30°, 45°, 60°
- For each ray we consider different spatial resolution: 1 pixel (0R), 1 radius (1R), 3 radiuses (3R)

Model

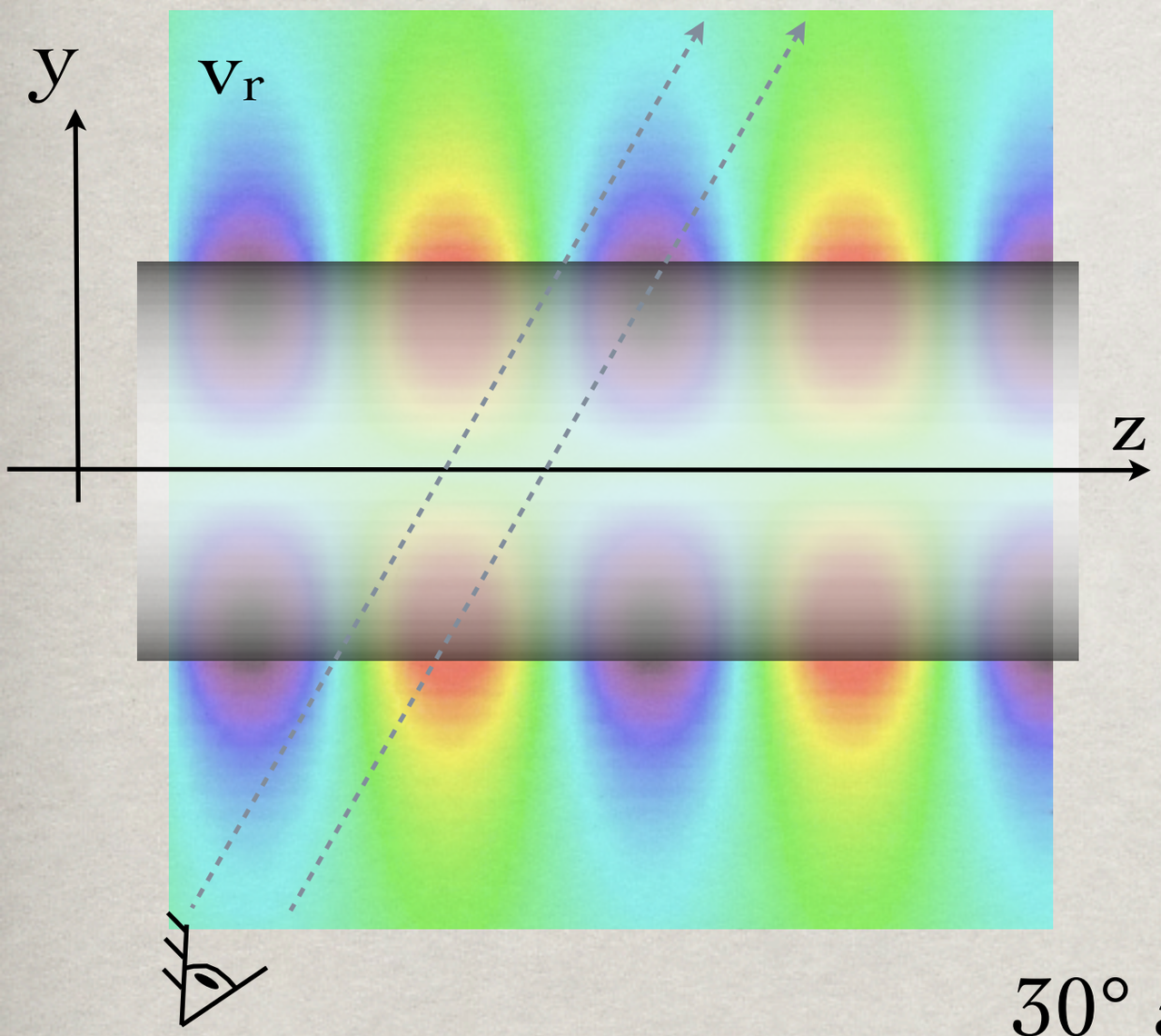

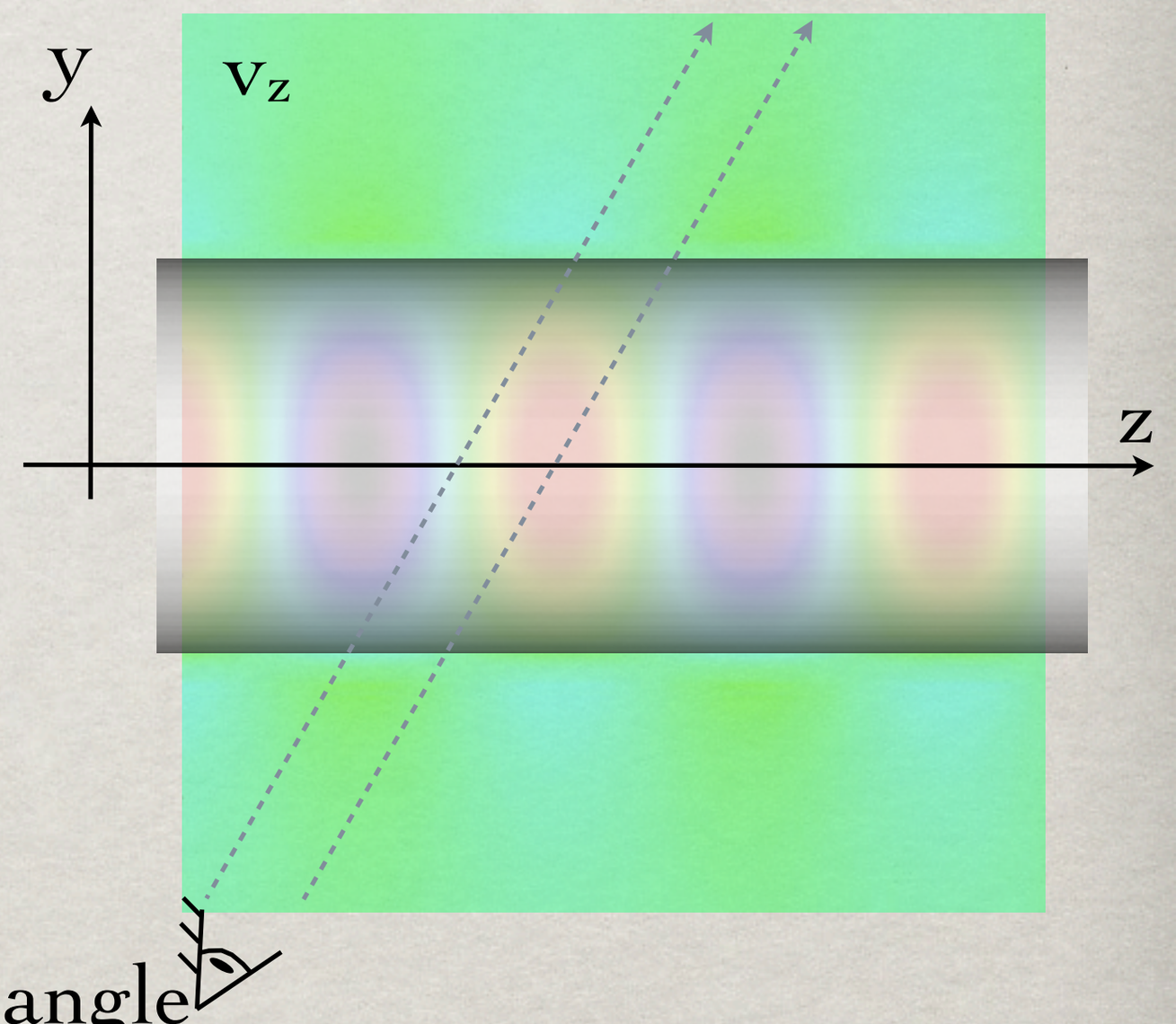

30° angle

- Different viewing angles (rays): 0°, 30°, 45°, 60°
- For each ray we consider different spatial resolution: 1 pixel (0R), 1 radius (1R), 3 radiuses (3R)

Model

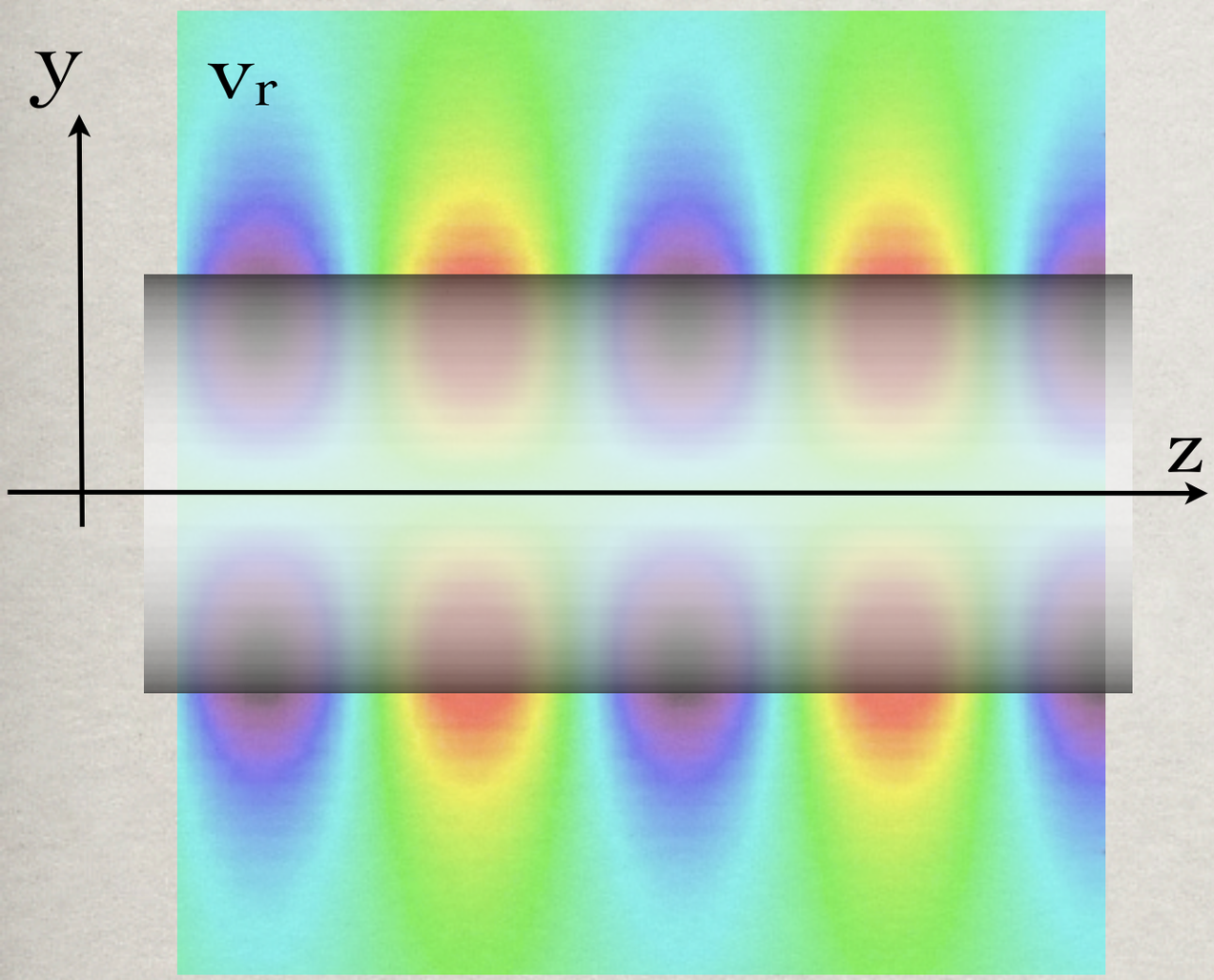

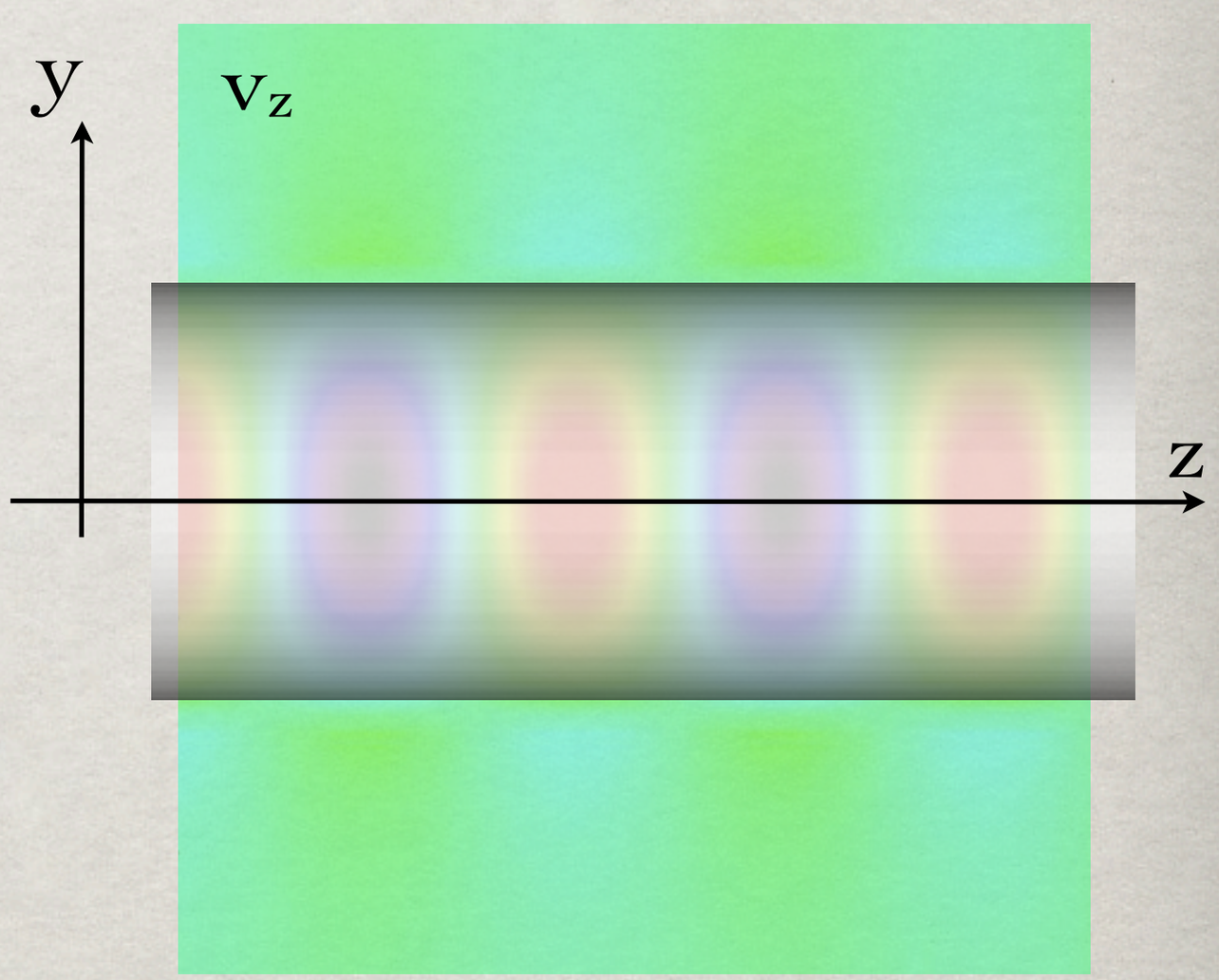

- Different viewing angles (rays): 0°, 30°, 45°, 60°
- For each ray we consider different spatial resolution: 1 pixel (0R), 1 radius (1R), 3 radiuses (3R)

Model

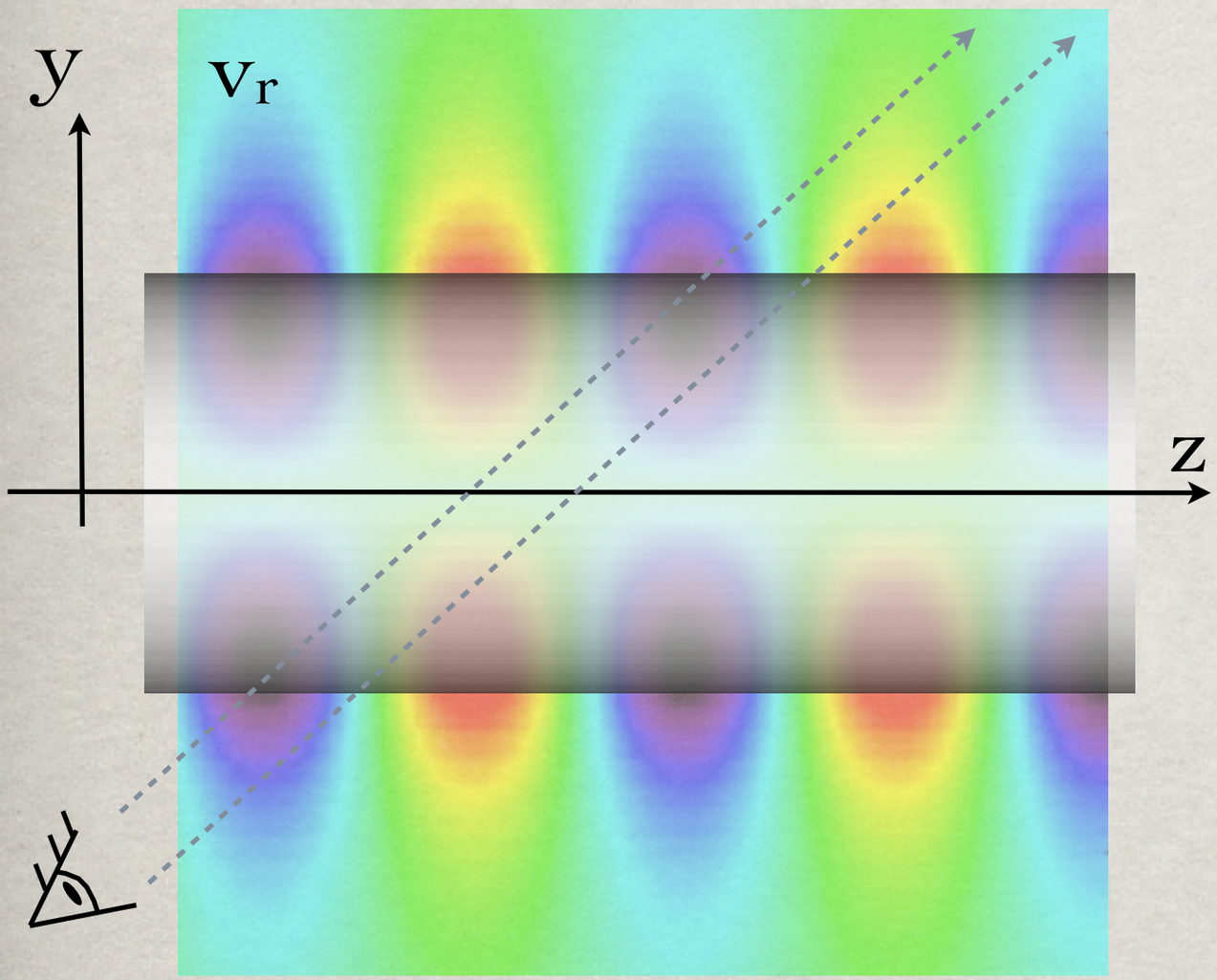

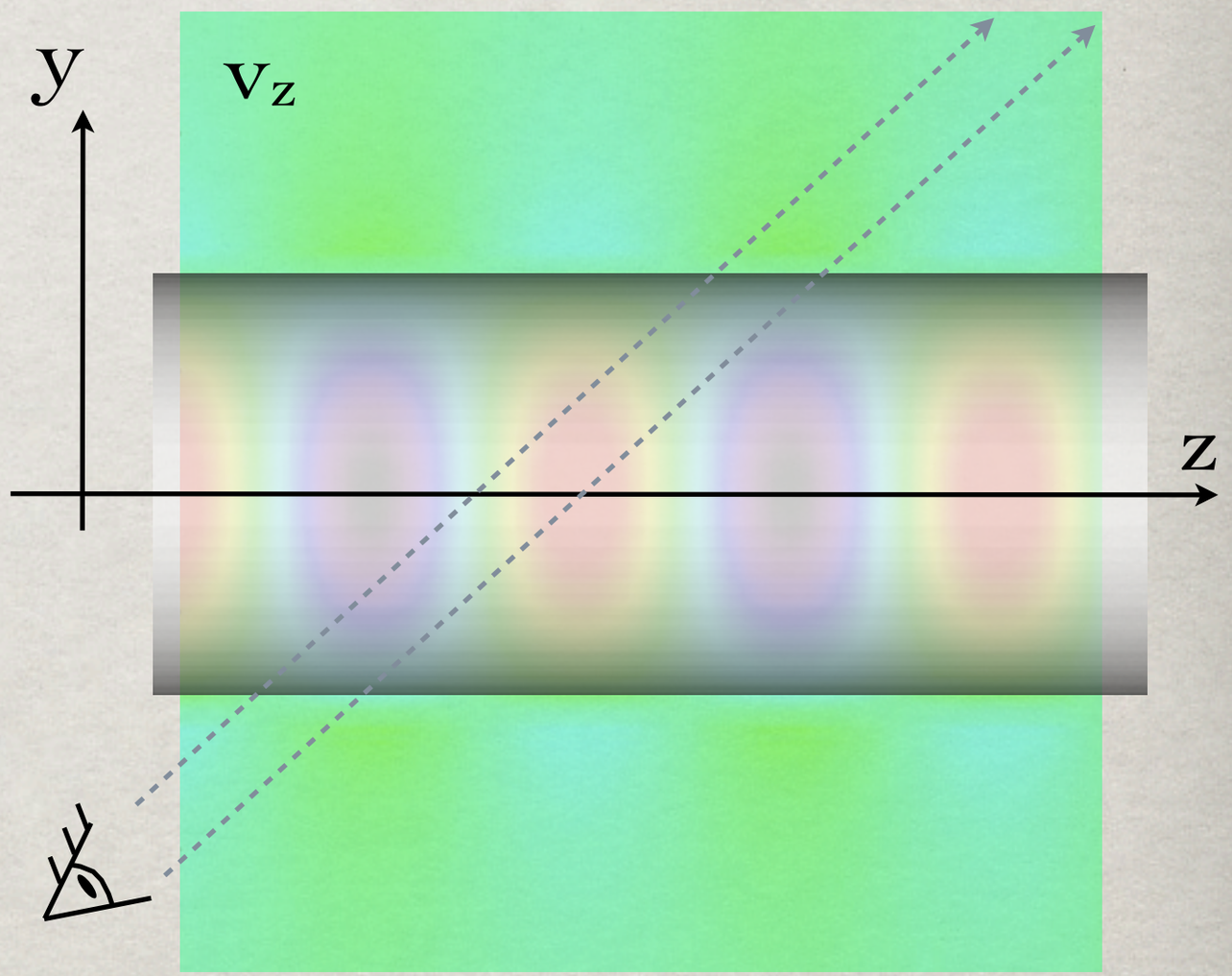

45° angle

- Different viewing angles (rays): 0°, 30°, 45°, 60°
- For each ray we consider different spatial resolution: 1 pixel (0R), 1 radius (1R), 3 radiuses (3R)

Model

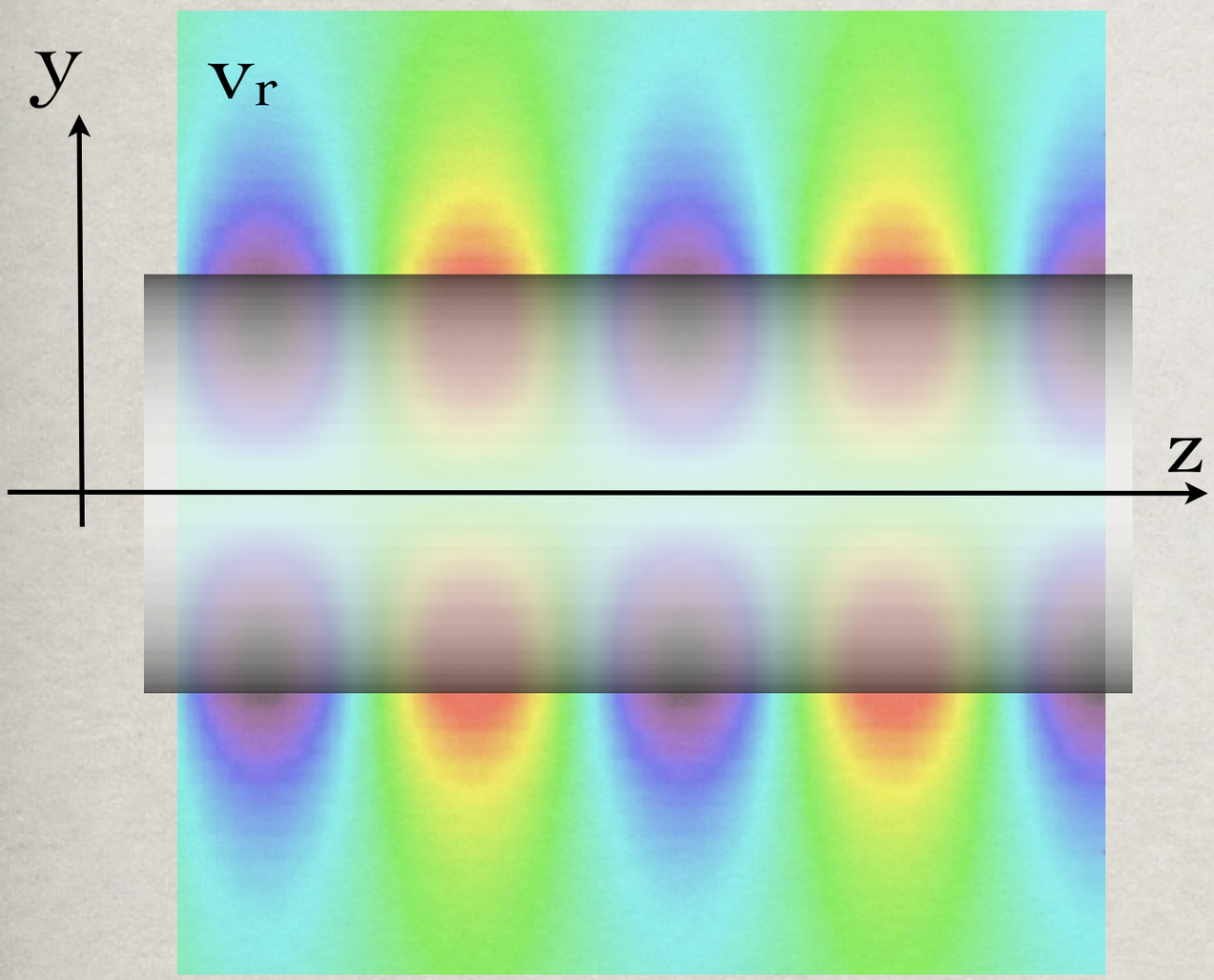

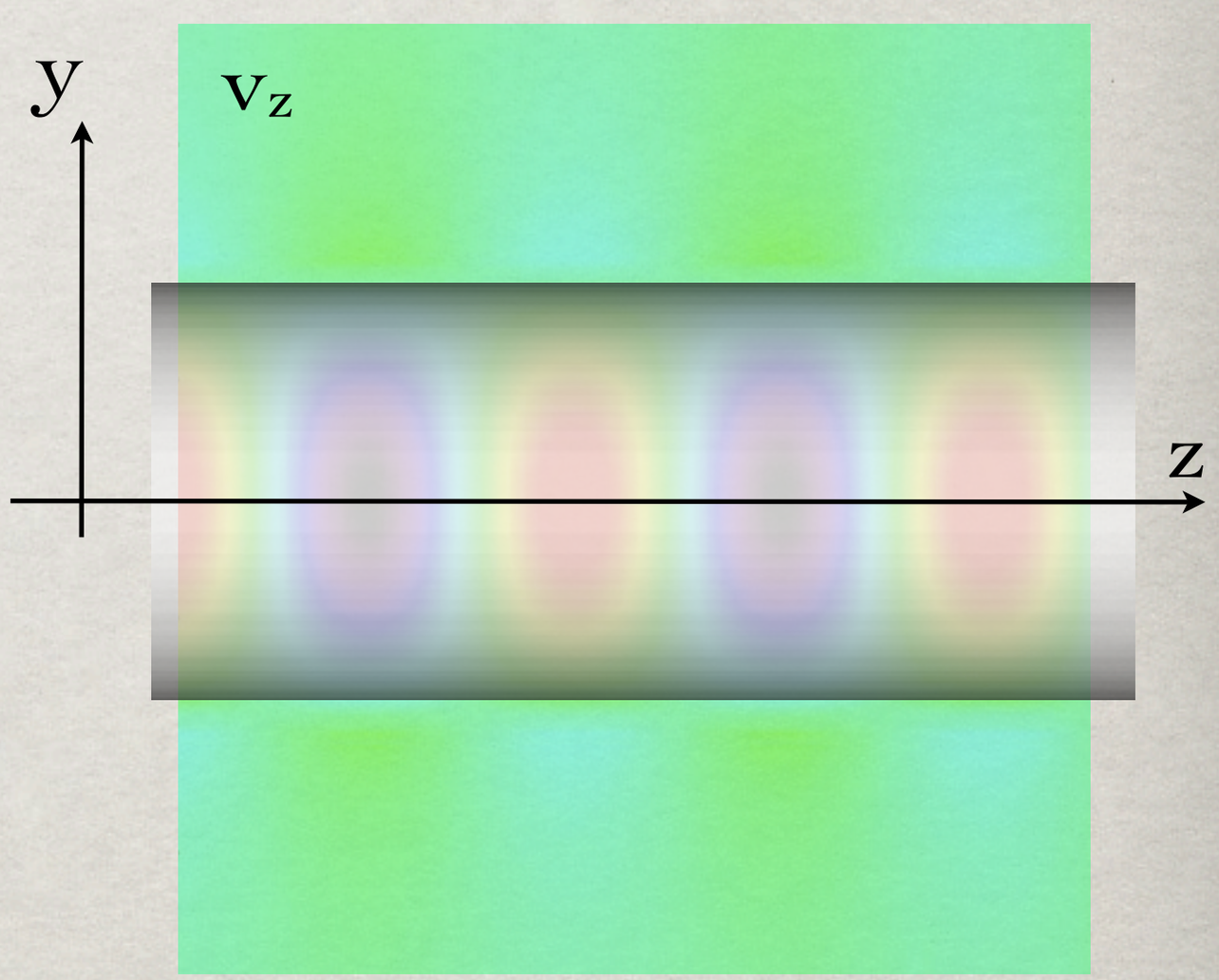

- Different viewing angles (rays): 0°, 30°, 45°, 60°
- For each ray we consider different spatial resolution: 1 pixel (0R), 1 radius (1R), 3 radiuses (3R)

Model

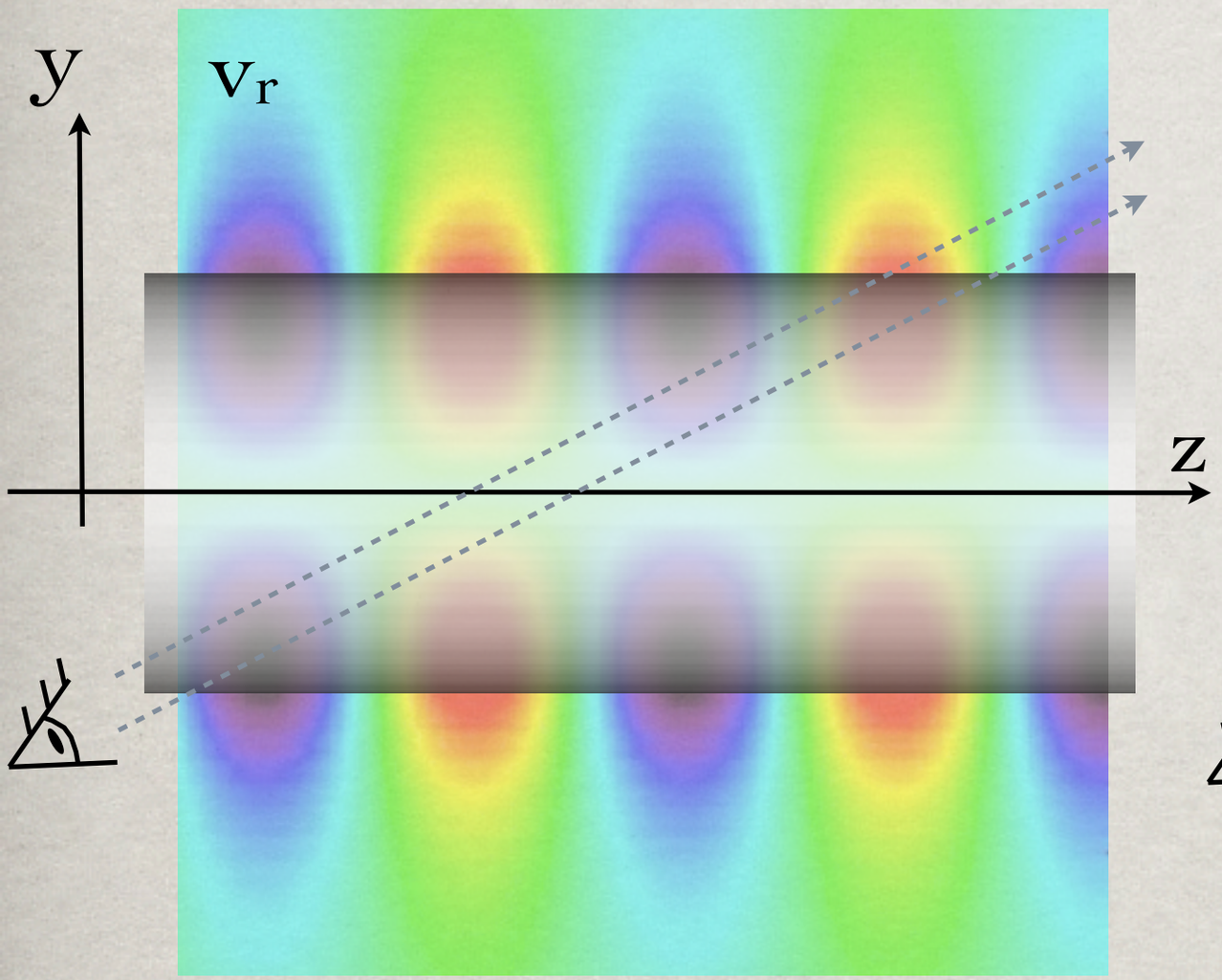

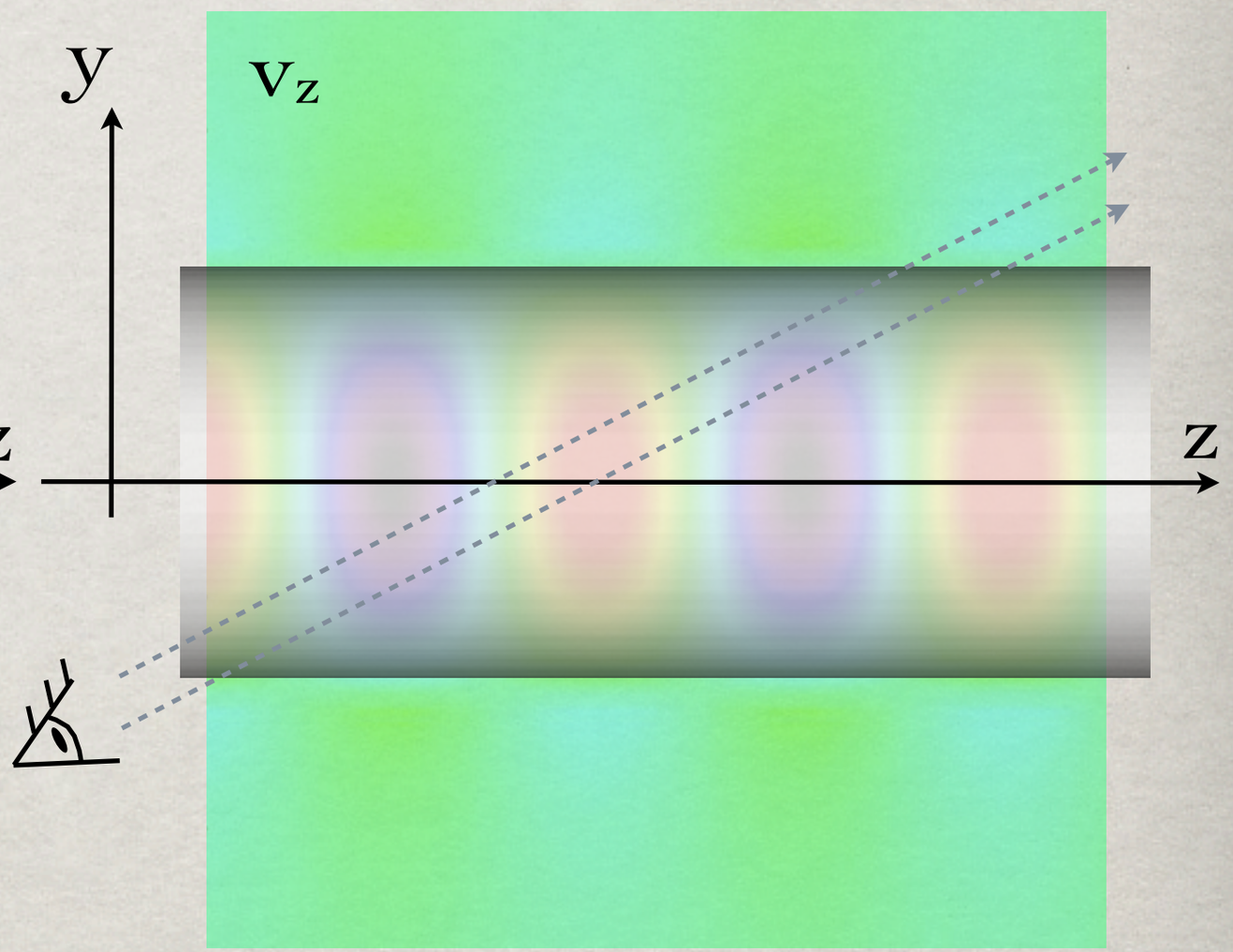

60° angle

- Different viewing angles (rays): 0°, 30°, 45°, 60°
- For each ray we consider different spatial resolution: 1 pixel (0R), 1 radius (1R), 3 radiuses (3R)

Model

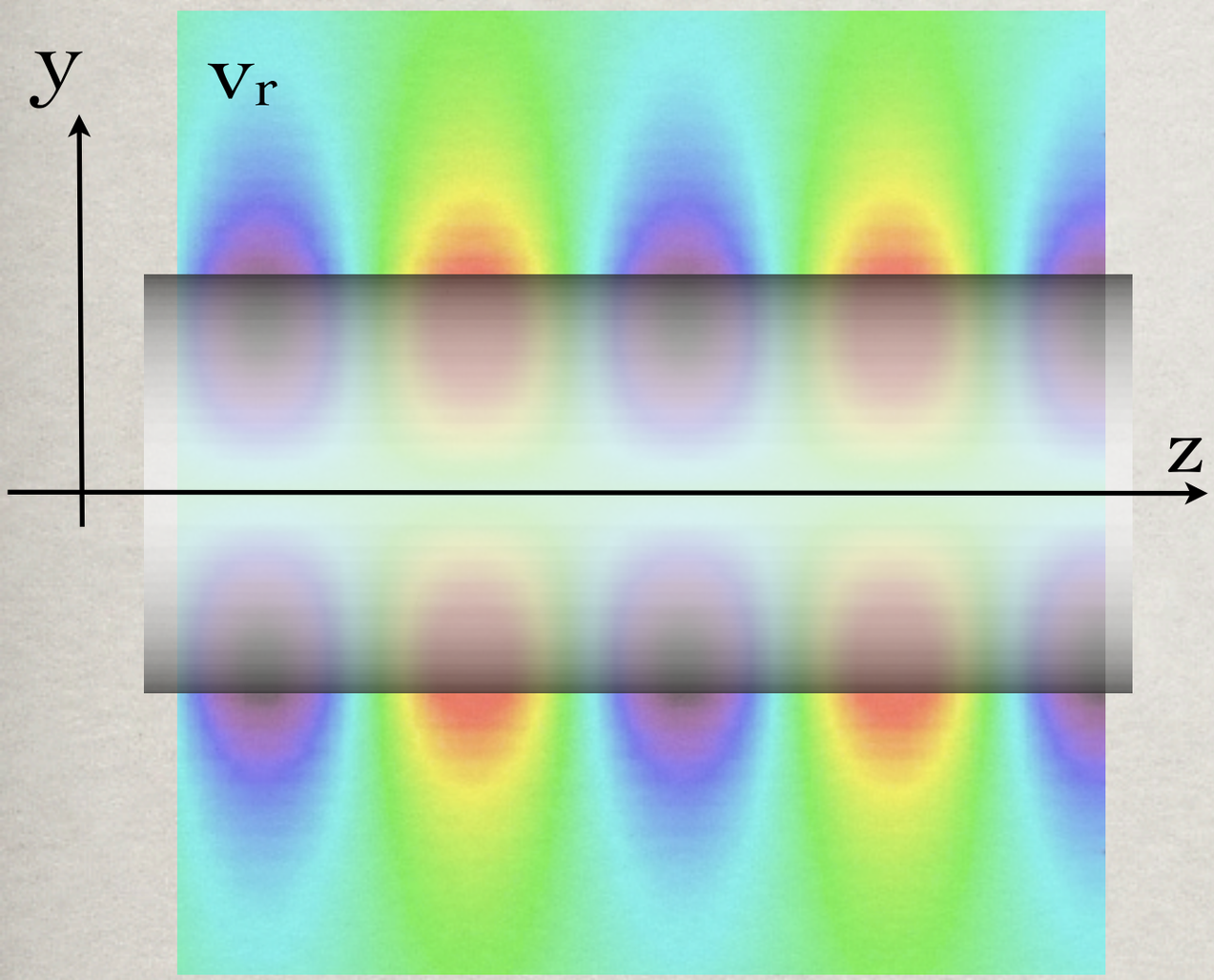

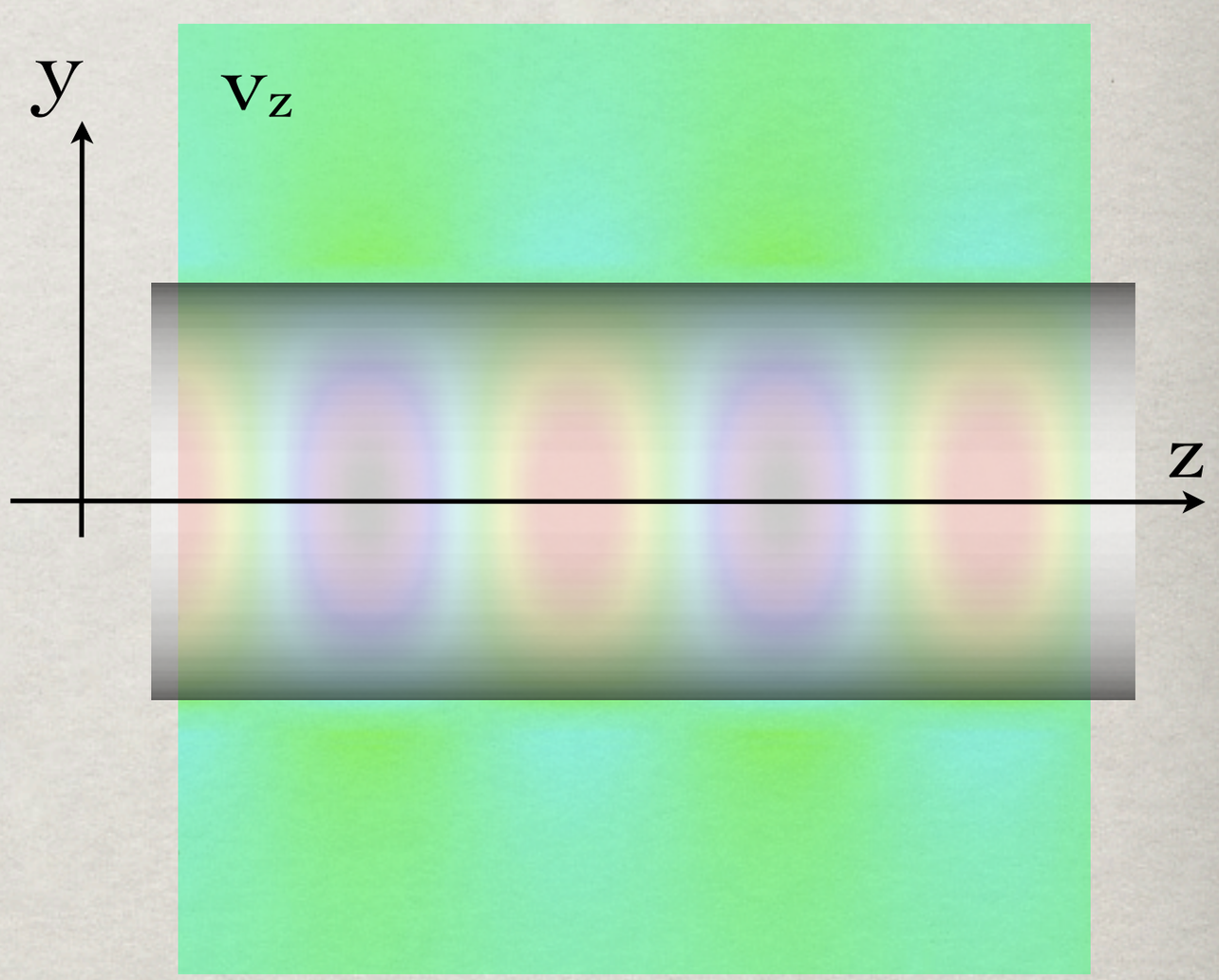

- Different viewing angles (rays): 0°, 30°, 45°, 60°
- For each ray we consider different spatial resolution: 1 pixel (0R), 1 radius (1R), 3 radiuses (3R)

Results - Imaging

Integrated emission along l.o.s. for different viewing angles

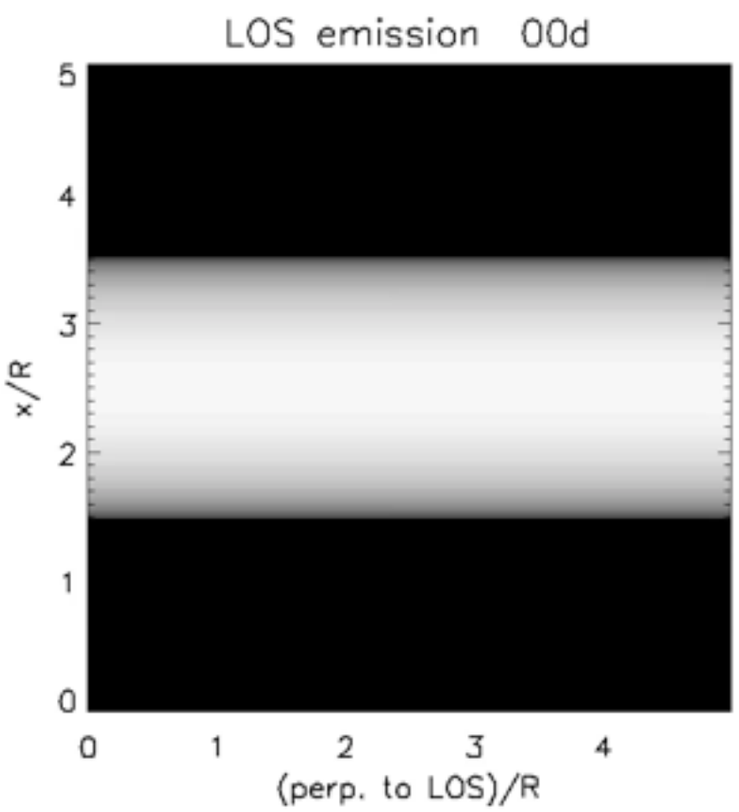

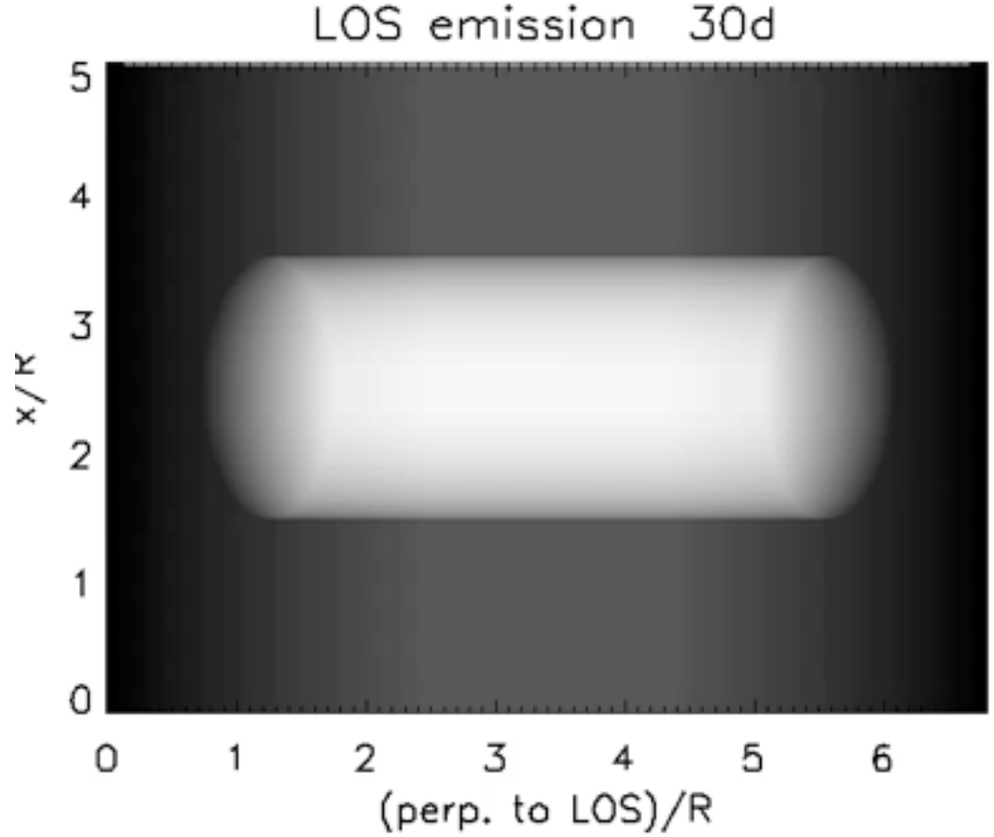

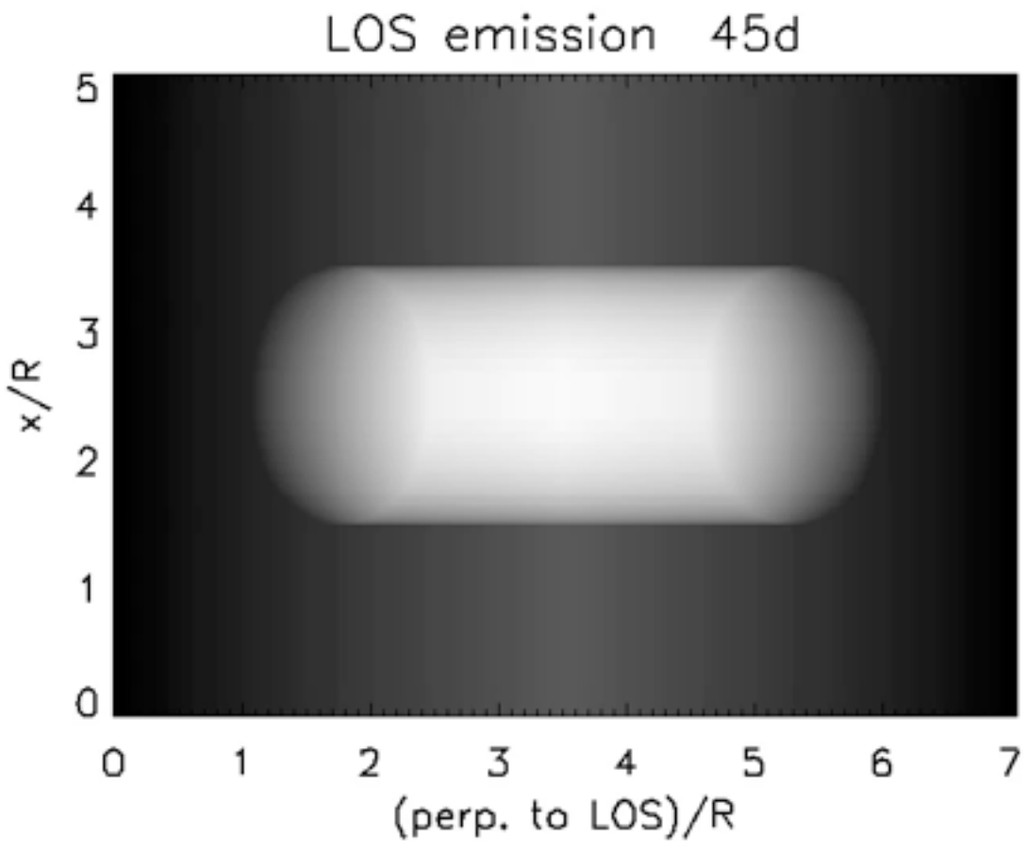

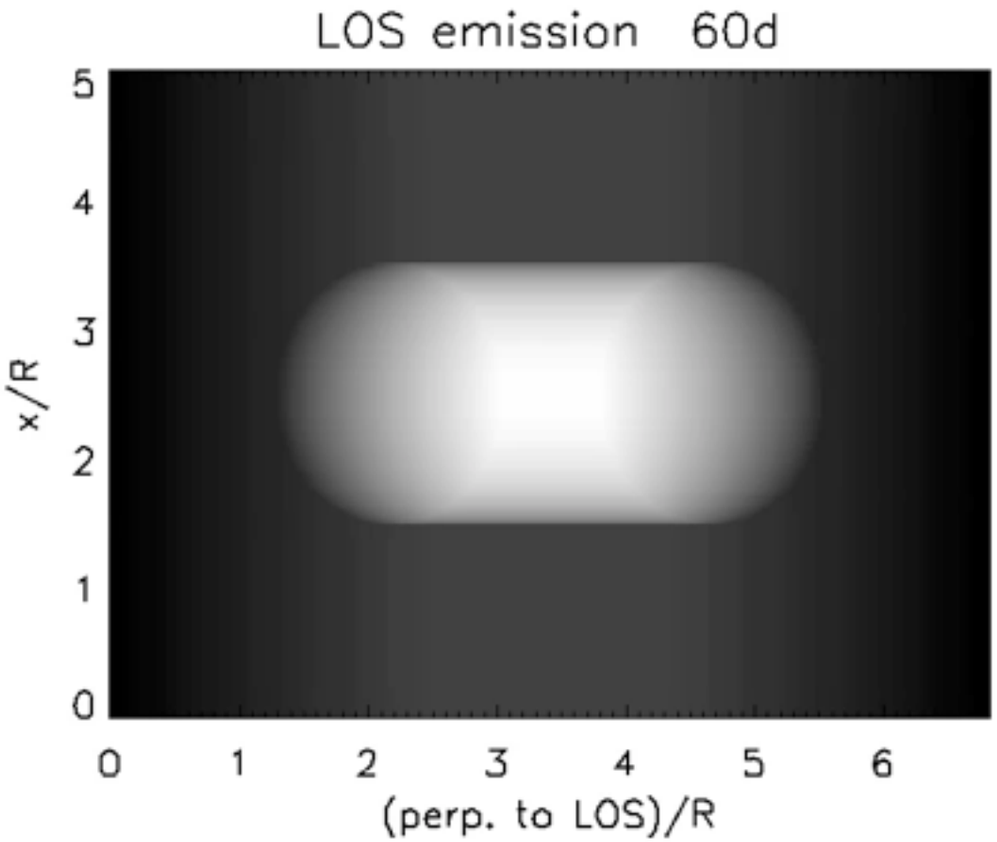

Results - imaging

integrated emission along rays

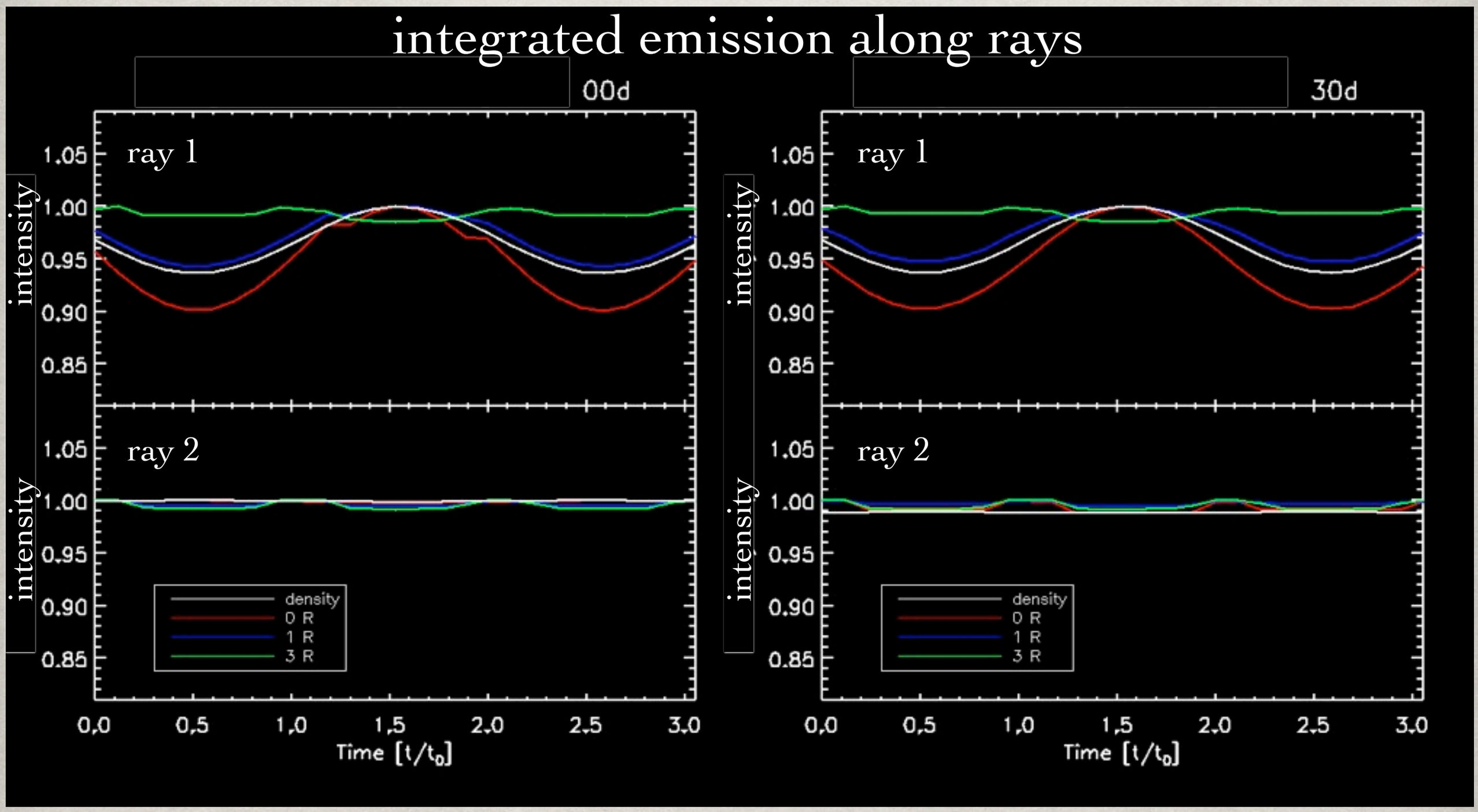

Intensity variations < 10% and decrease with resolution (Gruszecki et al. 2012): ray crosses >1 wavelength.

Results - imaging

integrated emission along rays

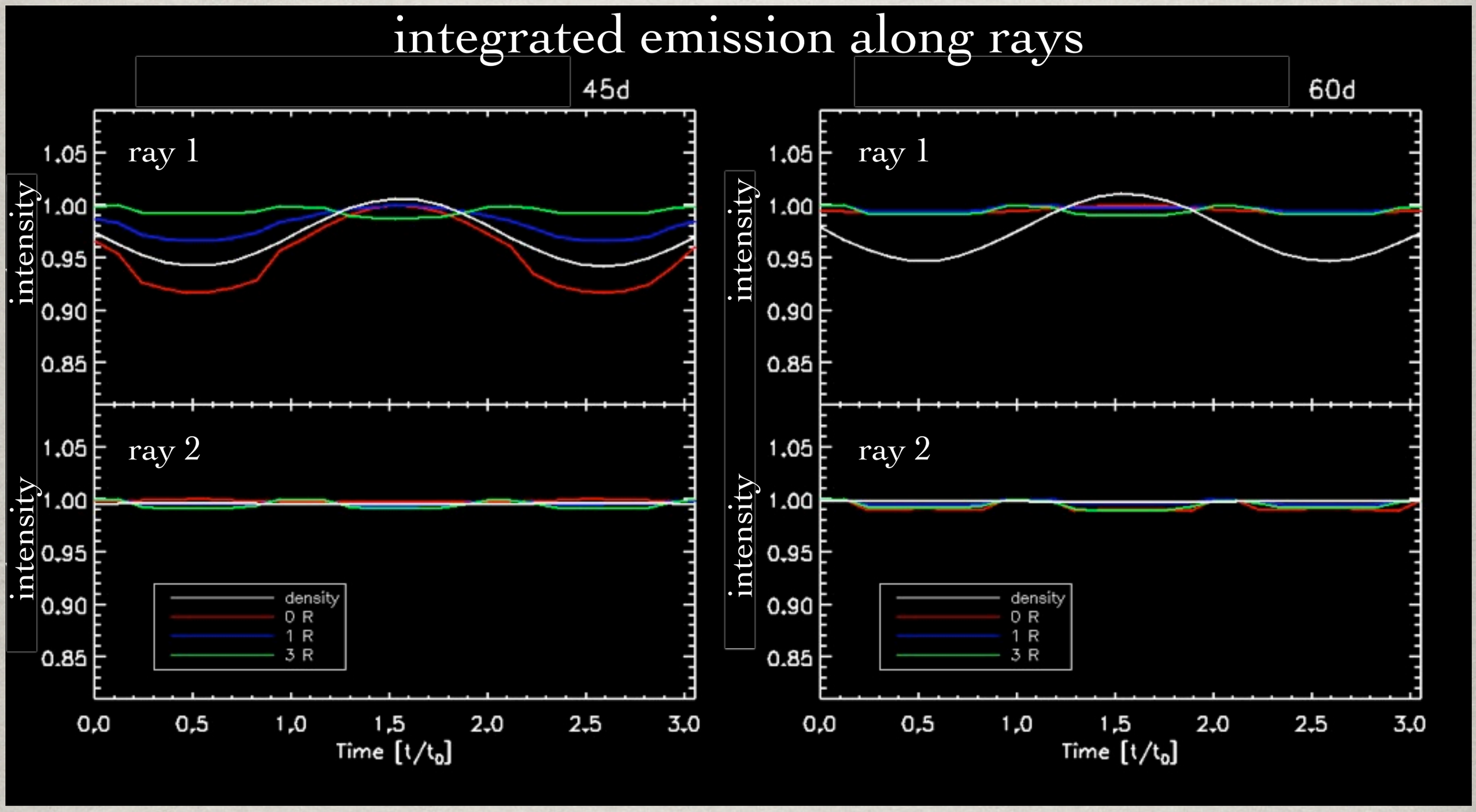

- The effect is more dramatic for larger viewing angles.
- For resolution up to 1R and angles up to 45° the emission variation along z is noticeable.

Results - spectroscopic

0° angle

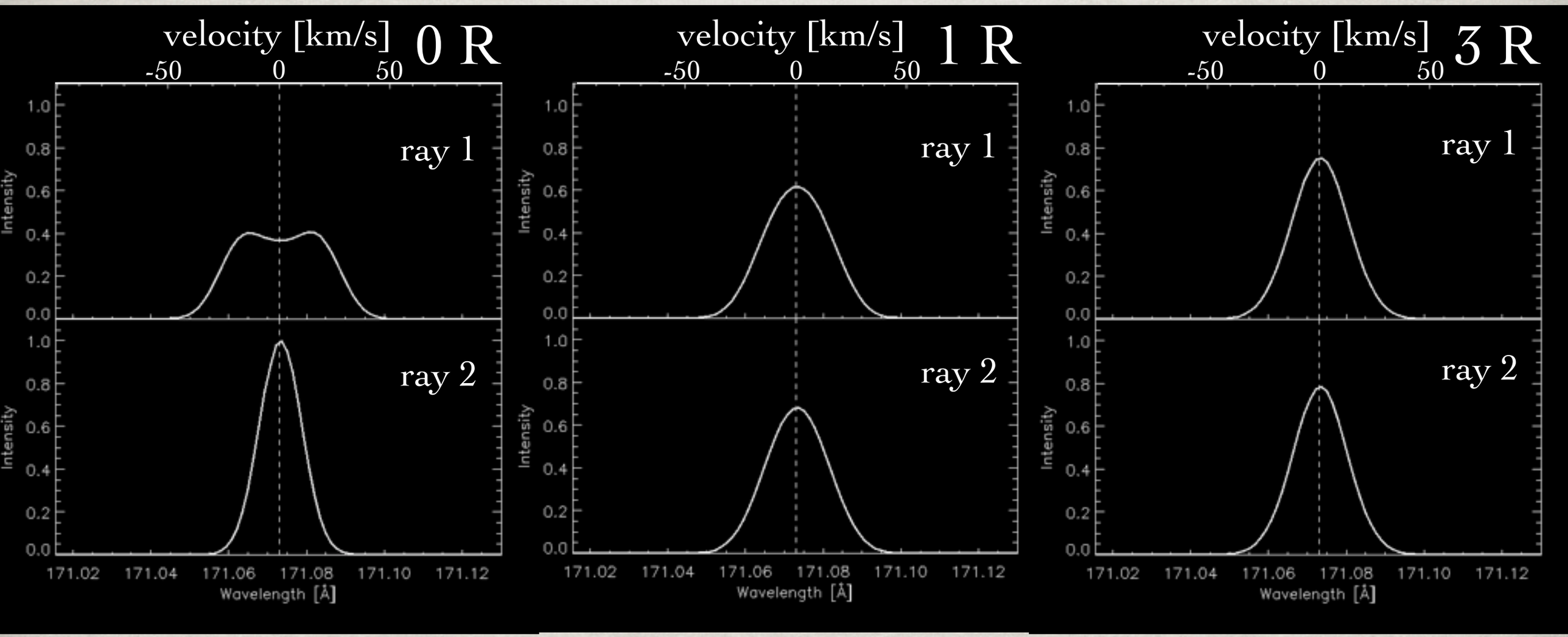

- Double peak for high resolution
- Periodic non gaussianity for low resolution, irrespective of ray crossing location

Results - spectroscopic

30° angle

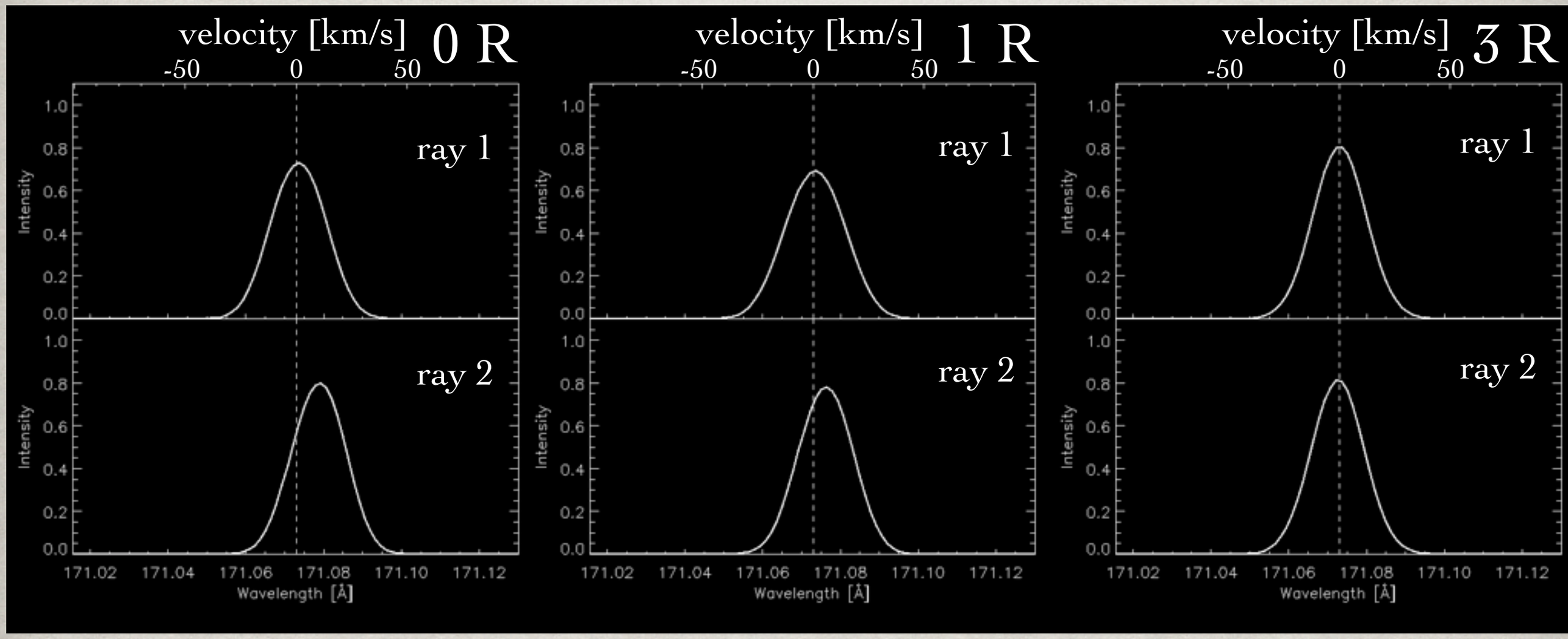

- Periodic blueshift and redshift excursions up to 1R resolution.
- Dependent on ray crossing location

Results - spectroscopic

45° angle

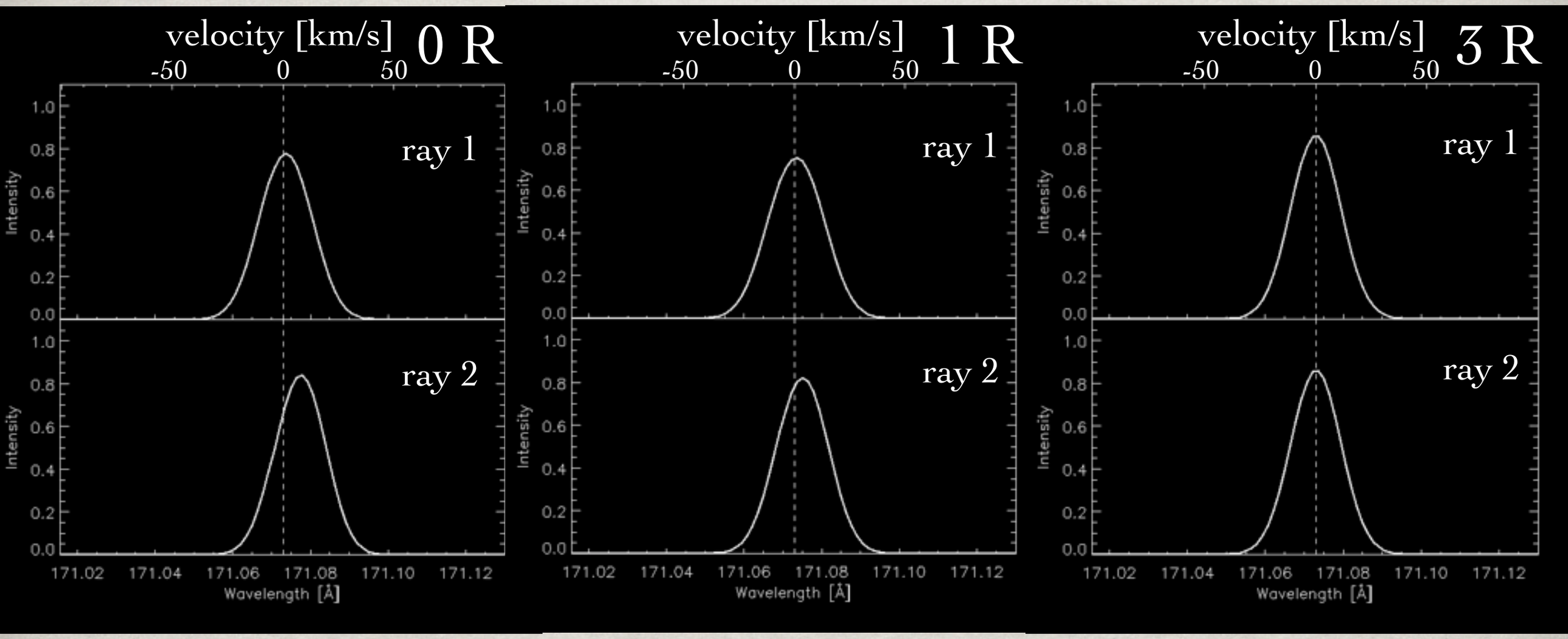

- Effect perdures for viewing angles up to 45°

Results - spectroscopic

60° angle

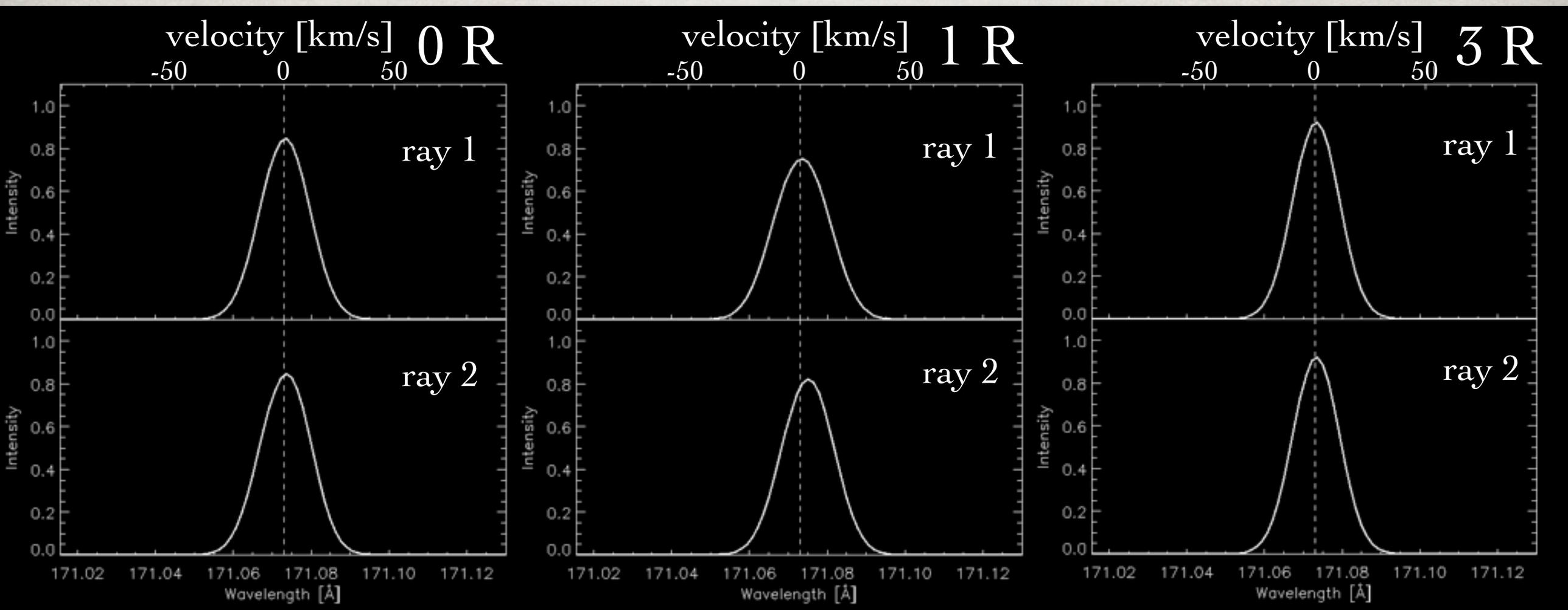

Conclusions

- Line-of-sight geometrical effects for a tube oscillating with the sausage mode: angle & resolution
- For imaging instruments:
  - Observable periodic intensity variations (< 10%) for spatial resolutions up to 1R and viewing angles up to 45°
  - Significant intensity variation along tube axis matching nodal structure of the standing wave
- For spectroscopic instruments:
  - Periodic non-gaussianity irrespective of viewing location and resolution (up to 3R)
  - Periodic blueshift and redshift excursions up to 1R resolution when viewing at an angle (up to 45°). Effect depends on viewing location along the tube.